Journal of Molecular Diagnostics, Vol. 12, No. 5, September 2010

DOI: 10.2353/jmoldx.2010.090187

Accurate Molecular Classification of Renal Tumors Using MicroRNA Expression

Eddie Fridman,*† Zohar Dotan,†‡ Iris Barshack,*† Miriam Ben David,§ Avital Dov,§ Sarit Tabak,§ Orit Zion,§ Sima Benjamin,§ Hila Benjamin,§ Hagit Kuker,* Camila Avivi,* Kinneret Rosenblatt,* Sylvie Polak-Charcon,*† Jacob Ramon,†‡ Nitzan Rosenfeld,§ and Yael Spector§

From the Departments of Pathology, and Urology,‡ Sheba Medical Center, Ramat-Gan; the Sackler School of Medicine,† Tel Aviv University, Tel Aviv; and Rosetta Genomics Ltd.,§ Rehovot, Israel*

Subtypes of renal tumors have different genetic backgrounds, prognoses, and responses to surgical and medical treatment, and their differential diagnosis is a frequent challenge for pathologists. New biomarkers can help improve the diagnosis and hence the management of renal cancer patients. We extracted RNA from 71 formalin-fixed paraffin-embedded (FFPE) renal tumor samples and measured expression of more than 900 microRNAs using custom microarrays. Clustering revealed similarity in microRNA expression between oncocytoma and chromophobe subtypes as well as between conventional (clear-cell) and papillary tumors. By basing a classification algorithm on this structure, we followed inherent biological correlations and could achieve accurate classification using few microRNAs markers. We defined a two-step decision-tree classifier that uses expression levels of six microRNAs: the first step uses expression levels of hsa-miR-210 and hsa-miR-221 to distinguish between the two pairs of subtypes; the second step uses either hsa-miR-200c with hsa-miR-139-5p to identify oncocytoma from chromophobe, or hsa-miR-31 with hsa-miR-126 to identify conventional from papillary tumors. The classifier was tested on an independent set of FFPE tumor samples from 54 additional patients, and identified correctly 93% of the cases. Validation on qRT-PCR platform demonstrated high correlation with microarray results and accurate classification. MicroRNA expression profiling is a very effective molecular bioassay for classification of renal tumors and can offer a quantitative standardized complement to current methods of tumor classification. ***(J Mol Diagn 2010, 12:687–696; DOI: 10.2353/jmoldx.2010.090187)***

Renal cancers account for more then 3% of adult malignancies and cause more than 13,000 deaths per year in the United States alone.[1] The incidence of renal cancers in the United States rose more than 50% between 1983 and 2002,[2] and the estimated number of new cases per year in the United States rose from 38,890 in 2006[3] to 54,390 in 2008.[1] Despite the trend of increased incidence of relatively small and kidney-confined disease, the rate of mortality has not changed significantly during the last two decades in the United States and Europe.[2,4–7] In the 1980s, renal tumors were basically regarded as one disease: the higher the stage and the grade, the worse the prognosis. After the 1980s, molecular biologists and pathologists described new entities with different morphological and biological characteristics. Evidence for different long-term prognosis for these subtypes makes the correct pathological diagnosis of a renal cancer critically important for the clinician.[8–11] Currently, it is well accepted that renal cell carcinoma (RCC) is a family of carcinomas that arise from the epithelium of the renal tubules.[12] The current classification of renal cell carcinoma includes four main types: conventional (clear cell), papillary, chromophobe, and collecting duct carcinoma, as well as unclassified renal cell carcinoma.[13] Oncocytoma, papillary adenoma, mesonephric adenoma, and angiomyolipoma are the main benign neoplasms in the kidney.

These different histological subtypes of RCC vary in their clinical courses and their prognosis, and different clinical strategies have been developed for their management. Patients with conventional RCC have a poorer prognosis, and differences may also exist between the prognosis of patients with papillary or chromophobe RCC.[8–11] The histological types arise through different constellations of genetic alterations and show expression or mutation in different oncogenic pathways; they therefore offer different molecular candidates for targeted therapy (eg, mTOR, VEGF, KIT).[14–16] Initial studies show

E.F., Z.D., and I.B. contributed equally to this study.

Accepted for publication March 29, 2010.

Authors affiliated with Rosetta Genomics are full-time employees and/or hold equity in the company, which develops microRNA-based diagnostic products and may stand to gain by publications of these findings. Authors from Sheba Medical Center and Tel Aviv University declare no financial conflict of interest.

Current address for N.R.: Molecular and Computational Diagnostics Laboratory, Cancer Research UK Cambridge Research Institute, Li Ka Shing Centre, Cambridge, UK; and Department of Oncology, University of Cambridge, Cambridge, UK.

Address reprint requests to Nitzan Rosenfeld, Ph.D., Rosetta Genomics Ltd, Plaut 10, Rehovot 76706, Israel. E-mail: nitzan.rosenfeld@cancer.org.uk.

differences in the responses of RCC subtypes to targeted therapies,[16,17] and future therapies are likely to be individualized for the different types.[15] The correct identification of these subtypes is therefore important for choice of treatment and for the selection of patients for clinical trials.[16,18]

Conventional RCC is the most frequent subtype of RCC and accounts for 60 to 70% of cases, thus causing the majority of renal cell cancer specific mortality. The term "conventional" is used to replace the name "clear cell," because some types have eosinophilic cytoplasm, generating a more difficult diagnostic challenge. In tumors of this type, a characteristic vascular network is commonly observed. The conventional carcinoma type is associated with germ line and somatic mutations of the von Hippel–Lindau (VHL) suppressor gene, and such mutations may indicate a more favorable prognosis.[19,20] Papillary RCC typically consists of a central fibrovascular core with epithelial covered papillae. It is subclassified into type 1 and 2 tumors that differ in terms of morphology, genotype, and clinical outcome.[21] Genetically, this type of tumor is associated with polysomies of chromosomes 7 or 17 and deficiency of Y.[22] Chromophobe renal cell carcinoma was included before 1986 in the group of conventional RCC. The typical form exhibits balloon cells with an abundant granular pale cytoplasm or eosinophilic cytoplasm that resemble the cells of oncocytoma.[23] Such features as described above are characteristic of the histological subtypes, but interobserver variations limit the accuracy of histological classification, with some types identified with a sensitivity of 70% or lower.[10] Furthermore, underlying biological mechanisms playing important roles in these tumors are yet to be elucidated.

Based on the growing clinical demand for accurate diagnosis of RCC subtypes, recent studies focused on the immunohistochemical profiling of different carcinomas. Allory et al lately described a subset of 12 antibodies as base for classification of renal cell carcinomas. In this report AMACR, CK7, and CD10 had the most powerful classification trees with 78–87% of carcinomas correctly classified.[24] Immunohistochemistry provides limited information for distinguishing chromophobe RCC from oncocytoma.[25,26] However, the increasing number of smaller tumors and needle-biopsy procedures places a strain on immunohistochemical methods. In a recent large study of 235 cases, more than 20% of the core needle biopsies were nondiagnostic.[27] This emphasized the need for developing additional types of molecular markers for the classification of renal tumors and for their study.

MicroRNAs, a family of small noncoding regulatory RNAs,[28] show promise as diagnostic biomarkers[29,30] thanks to their distinct expression profiles in tumors of different types and biological origins[31,32] and their chemical stability in clinical samples.[33] Their role in renal cancers and their potential as biomarkers for this family of malignancies are yet to be elucidated. One previous work studied the expression of 248 microRNA clusters in a set of 27 kidney specimens and found no association between microRNA expression and histological type.[34] A recent study compared expression of 470 microRNAs in 26 kidney samples and identified microRNAs differentially expressed between conventional and chromophobe renal tumors.[35] Another recent study using 20 RCC samples found correlation of microRNA expression to the histological type of the tumor and to prognosis of patients with clear cell RCC.[36] These studies included few samples and did not represent all of the major types of renal tumors. Here we report a study of microRNA expression profiles in more than 120 renal tumor samples. We identified microRNA biomarkers that are specifically expressed in the four most com-

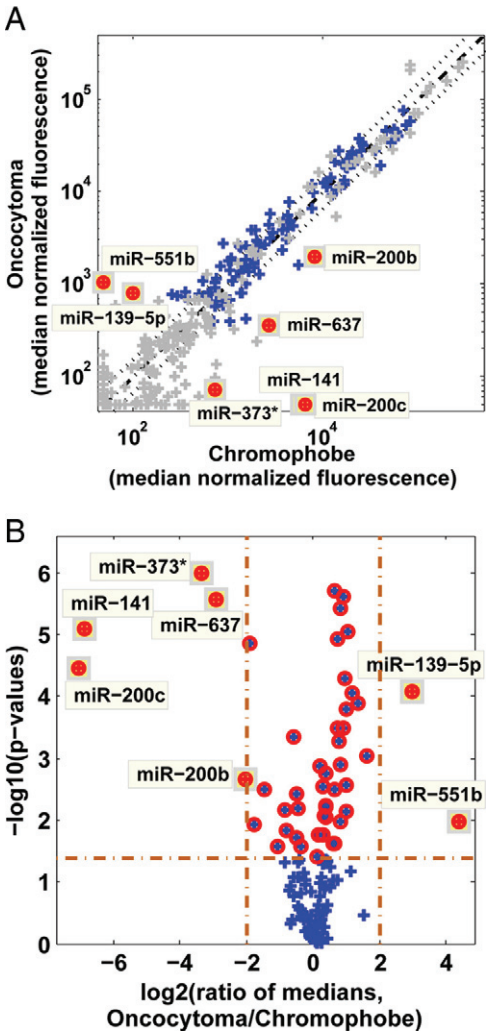

Figure 1. Graphic representations of differentially expressed microRNAs. **A:** Scatter-plot and volcano-plot comparison of oncocytoma and chromophobe samples from the training set. Median normalized fluorescence of oncocytoma samples (n = 21) is plotted against the median normalized fluorescence of chromophobe samples (n = 13). Each microRNA is represented by a blue cross. Control probes and microRNAs that did not pass the minimum expression threshold of median normalized fluorescence >700 (in at least one of the two groups) are shown in gray. Diagonal line shows equal signals (dash-dot line) and twofold change in either direction (dotted lines). MicroRNAs that had a fold change >4 in either direction and had a P value lower than 0.0417 (the threshold determined for a false discovery rate of 0.1 or lower) are shown as full red circles. **B:** Volcano plot showing the –log10(P value) against the log2 of the ratio of the median expression for the same data. MicroRNAs with strong fold changes have a large absolute value of the log2(ratio). Vertical lines indicate fourfold change in median signal in either direction; horizontal line indicates the P value cut-off of 0.0417. Red circles show p-value <0.0417; full circles as in panel A.

mon histological subtypes of renal tumors. We designed a microRNA-based classification algorithm that uses expression levels of 6 microRNAs to classify renal tumors. This classifier had an accuracy of 93% in histological classification of an independent test set of renal tumors.

Materials and Methods

Samples and RNA Extraction

One hundred twenty-five renal tumor formalin-fixed paraffin-embedded (FFPE) samples were obtained from the pathology archives of Sheba Medical Center (Tel-Hashomer, Israel, 107 samples) and commercial sources (ABS Inc., Wilmington, DE, and BioServe, Beltsville, MD, 18 samples). The study protocol was approved by the Research Ethics Board of each of the contributing institutes. FFPE samples were reviewed by a pathologist with experience in urological pathology (E.F.) for histological type based on hematoxilin-eosin (H&E) stained slides, performed on the first and/or last sections of the sample. Tumor classification was based on the World Health Organization (WHO) guidelines.[12] Tumor content was ≥80% for >80% of the samples, and samples with tumor content <60% were not used.

The differential microRNAs were identified and the classification algorithm was trained using 71 samples from 68 patients including 21 oncocytoma samples (from 18 patients; two available FFPE samples were used for each of three patients), 13 chromophobe RCC samples, 17 conventional RCC samples, and 20 papillary RCC samples. The classification algorithm was tested on an independent set of 54 samples from 54 new patients including 17 oncocytoma samples, 14 chromophobe RCC samples, 17 conventional RCC samples, and 6 papillary RCC samples.

Total RNA was isolated as previously described.[31,37] Briefly, seven to ten 10-μm-thick tissue sections were incubated a few times in xylene at 57°C to remove excess paraffin and then washed several times with ethanol. Proteins were degraded by incubating the sample in a proteinase K solution at 45°C for a few hours. RNA was extracted using acid phenol/chloroform and then precipitated using ethanol; DNAses were introduced to digest DNA. Total RNA quantity and quality was measured by Nanodrop ND-1000 (NanoDrop Technologies, Wilmington, DE).

Table 1. Differentially Expressed MicroRNAs

	Median values				(Conventional + papillary) versus (oncocytoma + chromophobe)			Chromophobe versus oncotcytoma			Papillary versus conventional		
MicroRNA name	Oncotcytoma	Chromophobe	Conventional	Papillary	*P* value	Fold	AUC	*P* value	Fold	AUC	*P* value	Fold	AUC
hsa-miR-141	50	5800	50	72	1.3E-03	14.38	0.67	8.0E-06	116.81	0.88	2.5E-01	1.45	0.64
hsa-miR-200c	**50**	**6500**	50	130	2.7E-03	11.84	0.68	**3.5E-05**	**129.68**	**0.88**	1.3E-01	2.61	0.66
hsa-miR-373*	72	730	84	79	2.7E-03	2.64	0.67	1.0E-06	10.23	0.92	5.6E-01	1.06	0.54
hsa-miR-637	350	2700	200	350	1.0E-03	2.25	0.71	2.7E-06	7.56	0.92	1.7E-01	1.76	0.65
hsa-miR-371-5p	420	1600	220	300	5.2E-04	2.26	0.75	1.4E-05	3.73	0.91	1.4E-01	1.36	0.66
hsa-miR-557	390	1100	150	210	6.3E-06	3.66	0.79	3.2E-03	2.72	0.79	3.0E-01	1.39	0.61
hsa-miR-193b	3900	1800	1200	670	2.6E-05	3.2	0.8	6.8E-02	2.2	0.68	3.0E-01	1.74	0.6
hsa-miR-365	2700	890	830	500	2.6E-04	2.49	0.78	9.2E-04	3.08	0.81	2.6E-02	1.67	0.7
hsa-miR-126	21000	14000	**29000**	**4200**	4.9E-03	1.68	0.66	3.3E-03	1.57	0.81	**5.0E-09**	**6.81**	**0.95**
hsa-miR-139-5p	**790**	**100**	120	50	2.7E-04	6.81	0.76	**8.6E-05**	**7.75**	**0.87**	1.6E-01	2.38	0.73
hsa-miR-222	52000	73000	5200	7500	4.1E-15	8.24	0.92	3.8E-03	1.42	0.74	6.3E-02	1.45	0.74
hsa-miR-221	**58000**	**81000**	**4000**	**8000**	**4.4E-17**	**10.95**	**0.93**	1.9E-02	1.39	0.74	1.1E-02	2	0.81
hsa-miR-221*	800	630	50	50	1.1E-17	14.39	0.94	1.3E-01	1.27	0.69	1.1E-01	1	0.6
hsa-miR-10a	37000	24000	6100	14000	9.0E-07	4.16	0.86	9.2E-02	1.53	0.73	5.7E-03	2.24	0.84
hsa-miR-30b	45000	59000	13000	19000	5.1E-11	2.69	0.9	2.8E-01	1.32	0.63	5.2E-03	1.5	0.76
hsa-miR-182	1400	1500	50	580	1.1E-06	5.8	0.81	8.1E-01	1.03	0.55	5.0E-04	11.66	0.81
hsa-miR-187	400	720	50	50	4.3E-06	9.13	0.81	4.9E-02	1.82	0.68	9.5E-01	1	0.51
hsa-miR-551b	1100	50	50	1300	2.8E-01	5.31	0.56	1.1E-02	21.1	0.75	2.1E-06	25.16	0.86
hsa-miR-138	50	50	70	790	3.9E-04	8.42	0.75	4.8E-01	1	0.6	1.7E-04	11.27	0.83
hsa-miR-31	50	330	**250**	**14000**	2.5E-06	29.31	0.81	1.5E-02	6.63	0.73	**2.5E-06**	**56.37**	**0.89**
hsa-miR-196b	430	210	370	1100	9.1E-02	1.53	0.63	4.1E-01	2.05	0.58	7.0E-02	2.81	0.72
hsa-miR-200a	1600	5500	3200	11000	3.5E-02	1.74	0.66	1.2E-02	3.38	0.82	8.0E-04	3.44	0.9
hsa-miR-200b	2000	8200	2800	15000	9.5E-02	1.85	0.63	2.2E-03	4.13	0.81	3.3E-05	5.17	0.91
hsa-miR-192	50	220	5200	1600	4.6E-08	21.24	0.84	5.4E-01	4.44	0.61	6.5E-02	3.28	0.74
hsa-miR-194	58	160	4200	2300	1.2E-07	20.63	0.83	4.2E-01	2.69	0.62	2.1E-01	1.87	0.69
hsa-miR-455-3p	120	98	1500	1200	1.8E-13	11.42	0.92	2.3E-01	1.27	0.58	2.0E-01	1.27	0.63
hsa-miR-146a	350	310	1400	1900	3.4E-12	4.98	0.92	7.0E-01	1.13	0.55	2.8E-01	1.38	0.64
hsa-miR-204	50	50	1700	2700	5.1E-10	48.33	0.87	9.9E-01	1	0.53	4.9E-02	1.59	0.71
hsa-miR-210	**280**	**370**	**11000**	**3300**	**1.2E-10**	**15.79**	**0.89**	9.2E-01	1.32	0.52	8.4E-03	3.38	0.89
hsa-miR-21	20000	21000	110000	180000	2.7E-10	7.79	0.88	4.4E-01	1.06	0.56	1.2E-01	1.56	0.68
hsa-miR-21*	50	66	800	2000	1.4E-12	28.66	0.91	4.3E-01	1.32	0.63	6.9E-02	2.45	0.78
hsa-miR-146b-5p	77	160	1700	1200	6.5E-12	10.4	0.9	5.0E-01	2.01	0.55	3.7E-01	1.38	0.58
hsa-miR-155	77	83	1300	600	9.2E-09	9.65	0.85	9.5E-01	1.08	0.5	5.4E-02	2.23	0.72

Pair-wise comparisons of each of the four histological types identified 33 differentially expressed microRNAs. Here we show the *P* value, fold-change of the median signal, and area under the ROC curve (AUC) for each of these microRNAs in comparing papillary with conventional tumors, oncocytomas with chromophobe tumors, and in comparing the combination of conventional with papillary with the union of chromophobe with oncocytoma. The six microRNAs used for classification are highlighted in bold and underline, along with their median values in the relevant histological types and the statistical parameters for the separation between the two types or groups (branches in the binary decision tree).

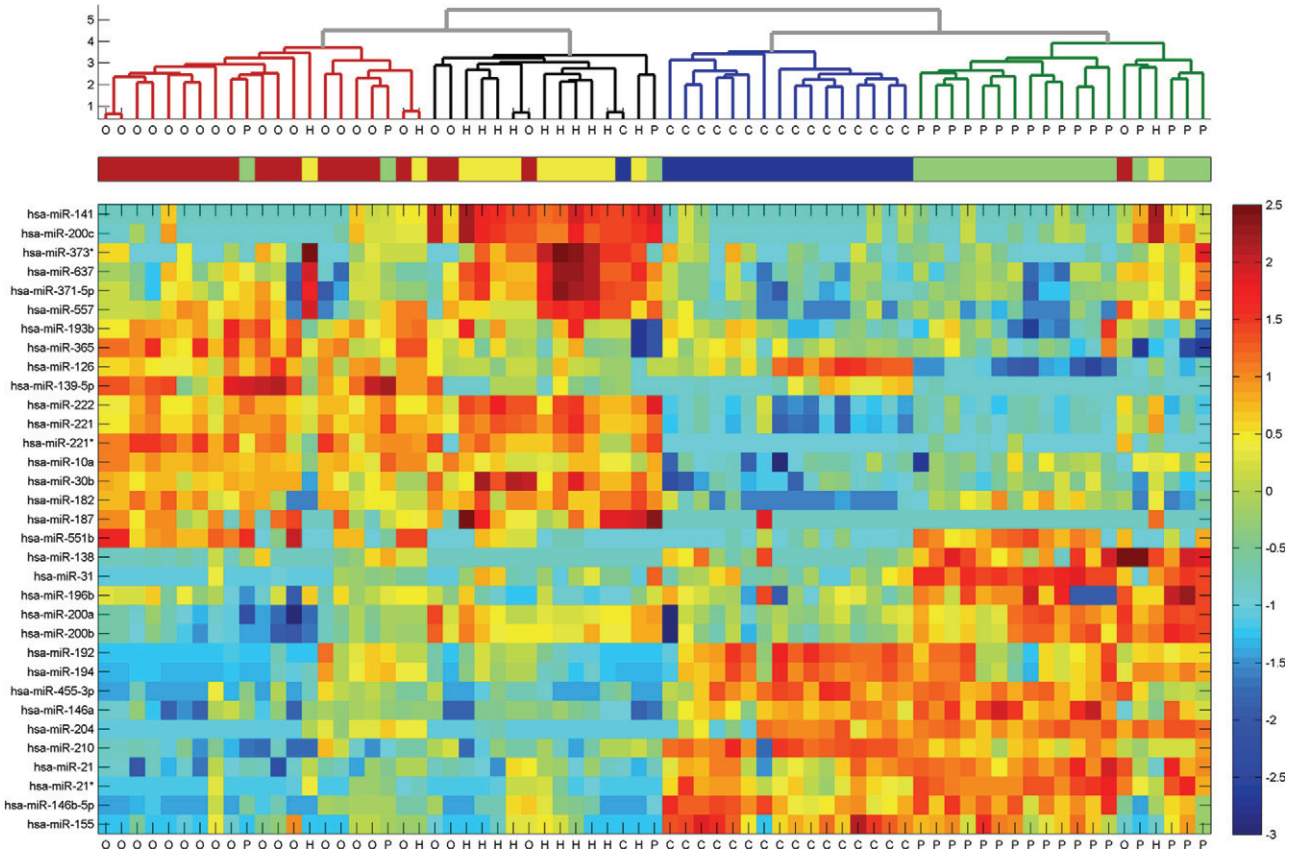

Figure 2. Clustering of kidney tumors by microRNA expression. The 33 differentially-expressed microRNAs (Table 1) were used to cluster the 71 samples of the training set. Normalized fluorescence signals were log-transformed, shifted to mean = 0, and rescaled to STD = 1 to enhance the expression differences. Outlying values were trimmed for optimal scaling (**lower panel**). The Euclidian distance was calculated between every pair of samples, and a hierarchical binary cluster tree was generated from these distances using the inner squared distance algorithm, and taking the logarithm of the resulting distances. The **upper panel** shows a dendrogram of hierarchical clustering of these samples. The histological type of each sample is indicated in the **middle panel**, with oncocytoma samples ("O," $n = 21$) indicated in red, chromophobe tumors ("H," $n = 13$) shown in yellow, conventional tumors ("C," $n = 17$) shown in blue, and papillary tumors ("P," $n = 20$) in green. The samples clustered into four groups that closely follow the four histological types. Among the four groups, the oncocytoma and chromophobe samples cluster together, whereas the conventional tumors show a higher degree of similarity to papillary tumors.

MicroRNA Profiling Using Microarrays

Custom microRNA microarrays were prepared as described previously.[31,37] Briefly on Slide E coated microarray slides (Schott Nexterion, Mainz, Germany) >900 DNA oligonucleotide probes representing microRNAs were spotted in triplicate using the BioRobotics MicroGrid II microarrater (Genomic Solutions, Ann Arbor, MI) according to the manufacturer's directions. Total RNA (3.5 μg) were labeled by ligation of an RNA-linker, p-rCrU-Cy/dye (Eurogentec Inc., San-Diego, CA; Cy3 or Cy5) to the 3′ end. Slides were incubated with the labeled RNA for 12–16 hours at 55°C and then washed twice. Arrays were scanned using Agilent DNA Microarray Scanner Bundle (Agilent Technologies, Santa Clara, CA) at a resolution of 10 μm with 100% and 10% laser power. Array images were analyzed using SpotReader software (Niles Scientific, Portola Valley, CA). Microarray spots were combined and signals normalized as described previously.[31,37]

Statistical Methods for Microarray Analysis

For every pair of groups (eg, oncocytoma versus chromophobe or conventional versus papillary), microRNA expression was compared for all microRNAs that had expression level above background (median normalized fluorescence signal >700) in at least one of the two groups. *P* values were calculated using a two-sided (unpaired) Student's *t*-test on the log-transformed normalized fluorescence signal (Figure 1, A and B). The threshold for significant differences was determined by setting a false discovery rate of 0.1, to correct for effects of multiple hypothesis testing,[38] resulting in *P* value cut-offs in the range of 0.03–0.06. For each differentially expressed microRNA we calculated the fold-difference (ratio of the median normalized fluorescence) and the area under curve (AUC) of the response operating characteristic (ROC) curve (Table 1). Hierarchical clustering was used to group histological types (Figure 2). For classification, two microRNAs with opposite specificity (Figure 3) were chosen at each decision point (Figure 4A), and their ratio of expression (ratio of the normalized fluorescence signal) was calculated for each sample. A threshold level for the value of the ratios was determined using the training set of samples (indicated by the gray shaded regions in Figure 4, B–D) by choosing the cut-off value with the smallest number of classification errors on the

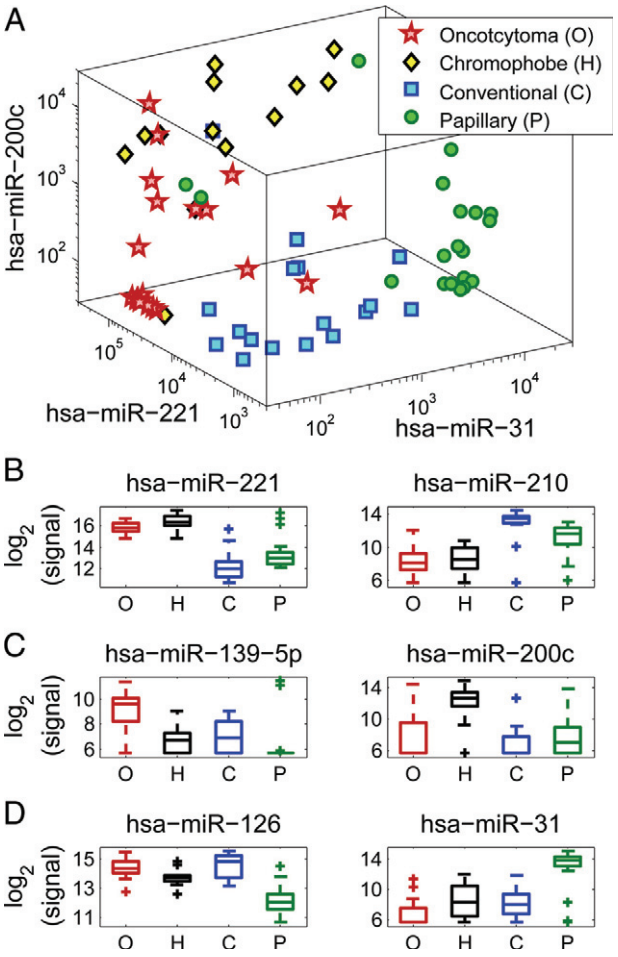

Figure 3. Separation between histological types using a small set of microRNAs. The training set included oncocytoma samples ("O," $n = 21$, red stars), chromophobe tumors ("H," $n = 13$, black/yellow diamonds), conventional tumors ("C," $n = 17$, blue squares), and papillary tumors ("P," $n = 20$, green circles). Plotting the expression of hsa-miR-221, hsa-miR-31, and hsa-miR-200c in each of the training set samples (**A**), the four types of samples group into areas with distinct ranges of expression. Box-plots (**B**, **C**, and **D**) indicate expression levels of microRNAs in the four histological types (same samples as in **A**), showing the median value (horizontal line), 25 to 75 percentile (box), extent of data (whiskers), and outliers (crosses). Hsa-miR-221 and hsa-miR-210 (**B**) have distinct expression in oncocytomas and chromophobe tumors compared with conventional and papillary tumor, with hsa-miR-221 more strongly expressed in oncocytomas and chromophobe tumors, and hsa-miR-210 more strongly expressed in conventional and papillary tumors. Hsa-miR-139-5p and hsa-miR-200c (**C**) have distinct expression in oncocytomas compared with chromophobe tumors, with hsa-miR-139-5p more strongly expressed in oncocytomas and hsa-miR-200c more strongly expressed in chromophobe tumors. Hsa-miR-126 and hsa-miR-31 (**D**) have distinct expression in conventional tumors compared with papillary tumors, with hsa-miR-126 more strongly expressed in conventional tumors and hsa-miR-31 more strongly expressed in papillary tumors.

training set. These thresholds were used to classify the test samples.

qRT-PCR Validation

Six microRNA chosen for classification based on microarray results and U6 small RNA (used for normalization) were measured using a quantitative real-time polymerase chain reaction (qRT-PCR) method recently described.[33] Briefly, RNA was incubated in the presence of poly(A) polymerase (NEB), MnCl2, and ATP for 1 hour at 37°C. Then, using an oligodT primer harboring a consensus sequence, reverse transcription was performed on total RNA using SuperScript II RT (Invitrogen). Next, the cDNA was amplified by real-time PCR; this reaction contained a microRNA-specific forward primer, a TaqMan probe complementary to the 3′ of the specific microRNA sequence as well as to part of the polyA adaptor sequence, and a universal reverse primer complementary to the consensus 3′ sequence of the oligodT tail. The cycle threshold (Ct, the PCR cycle at which probe signal reaches the threshold), representing expression levels in logarithmic scale, was determined for each well.

Normalization of qRT-PCR Results

The normalized Ct of each microRNA in each sample [normCt(miR-X)] was determined according to the measured Ct of that microRNA, the Ct of U6 in the same sample and the global average Ct [ie, the average Ct measured in the experiment (globalAverageCt = 29.9)]:

$$\text{normCt(miR-X)} = 50 - [\text{Ct(miR}-\text{X)} - \text{Ct(U6)} + \text{globalAverageCt}]$$

Comparison of qRT-PCR and Microarray Results

The classification scheme determined using microarray results was used for analysis of qRT-PCR results. At each decision point (Figure 4), the expression ratio between the two microRNA according to qRT-PCR was calculated as the difference in normalized Ct (because Ct is in logarithmic scale, Ct differences represent ratios of expression). Correlation coefficients of microarray expression ratios and qRT-PCR expression ratios were calculated. Classification thresholds for qRT-PCR were determined based on the microarray results: for each decision point, the approximate qRT-PCR threshold was interpolated from the linear fit to the microarray data (Figure 5, A, C, and E). One correctly classified sample closest to the threshold was then chosen from each sample group. The average qRT-PCR expression ratio of these two samples was used as classification threshold of qRT-PCR results.

Results

One hundred twenty-five FFPE samples of renal tumors were collected, including 38 oncocytoma samples, 27 chromophobe RCC samples, 34 conventional (clear) cell RCC samples, and 26 papillary RCC samples. The initial sample set used for biomarker identification and for training a classifier (see below) included 71 samples. Total RNA was extracted from these samples, and microRNA expression was assessed using microarrays.

We first looked for microRNAs that are differentially expressed between different histological subtypes of kidney tumors. We compared the expression of microRNAs between oncocytoma samples ($n = 21$, from 18 patients), chromophobe tumors ($n = 13$), conventional tumors ($n =$

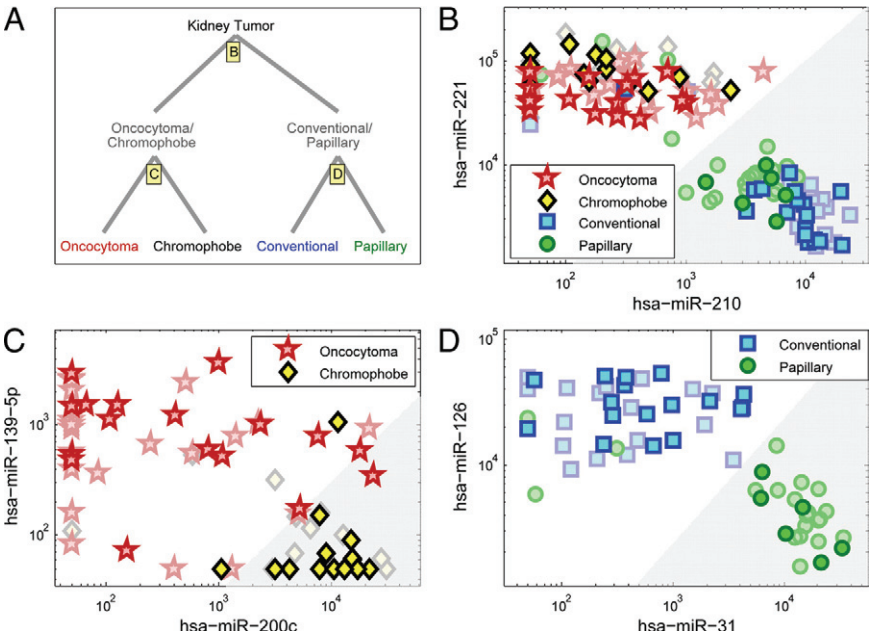

Figure 4. Classification of kidney tumors using expression levels of six microRNAs (microarray data). **A:** Classification proceeds in two steps, following the cluster structure of the histological types (Figure 2). First, samples are classified into either the oncocytoma/chromophobe pair, or the conventional/papillary pair, using expression levels of hsa-miR-210 and hsa-miR-221 (**B**). In the second step, oncocytoma is differentiated from chromophobe using expression levels of hsa-miR-200c and hsa-miR-139-5p (**C**), and conventional is differentiated from papillary using expression levels of hsa-miR-31 and hsa-miR-126 (**D**). Independent test samples included oncocytoma samples (n = 19, red stars), chromophobe tumors (n = 14, black/yellow diamonds), conventional tumors (n = 17, blue squares), and papillary tumors (n = 6, green circles). The gray shaded regions indicate the thresholds for classification for each pair of microRNAs, indicating in each case the right branch in the binary classification tree (**A**). The 71 samples that were used for training the thresholds (see Methods and Figure 3) are shown in faded symbols in the background.

17), and papillary tumors (n = 20). More than 900 microRNAs[39] were compared using statistical tests. MicroRNAs were considered differentially expressed between any two histological types if their t-test significance (P value) indicated a false discovery rate below 0.1 and their median expression level changed at least fourfold between the two groups (Figure 1). Thirty-three microRNAs were identified as differentially expressed between different kidney tumors types (Table 1). To identify underlying similarities between the histological types, the expression level of these 33 microRNAs was used to cluster the 71 samples. This analysis identified four main clusters that closely followed the predefined groups (Figure 2). Further, the expression of microRNAs showed a high degree of similarity between conventional and papillary tumors and between chromophobe RCC and oncocytoma, and a lower degree of similarity between these pairs (Figure 2), consistent with the known biology of these tumors.[14]

The clustering also identified groups of microRNAs with similar profiles. Such coregulated groups can hint at a possible effect of upstream regulatory components. An analysis of predicted binding sites of transcription factors near the start sites of coregulated microRNA transcripts[40] generates a list of transcription factors that may be enriched for factors related to biological differences between the histological types[40] (Table 2).

Given the underlying biological similarities between the tumor types (Figure 2), we decided to construct a classifier to identify kidney tumor subtype in two steps, following the binary structure[31] of the hierarchical clustering tree: the first step identifies whether the sample belongs to one pair of types (chromophobe, oncocytoma) or to the other pair (conventional, papillary); the second step decides between the two types in each pair. The classifier therefore has three decision points, corresponding to the comparisons in Table 1. For each such decision point (or "node"), we chose two microRNAs: one that is highly expressed in one group, and another that is more strongly expressed in the other group. MicroRNAs were selected based on their expression levels and distributions in the training set (Table 1), with the aim of selecting microRNAs that provide a distinct difference in expression that can be used for accurate classification.[30,37,41] For identifying between the pair of types (chromophobe, oncocytoma) and the pair (conventional, papillary), we chose hsa-miR-221 and hsa-miR-210; for identifying between chromophobe and oncocytoma, we chose hsa-miR-200c and hsa-miR-139-5p; and for identifying between papillary and conventional, we chose hsa-miR-31 and hsa-miR-126 (Figure 3). Using one microRNA from each set is sufficient to obtain a clear separation between the four groups (Figure 3A), but to provide internal normalization and ensure better performance we used a combination of two microRNAs with complementary specificities at each decision point. Among this set of microRNAs, each histological type has high expression of at least two microRNAs (eg, hsa-miR-210 and hsa-miR-31 for papillary, or hsa-miR-221 and hsa-miR-200c for chromophobe) and low expression of at least two other microRNAs (Figure 3).

We used the 71 samples of the training set to train a simple classifier, comprising two steps and three pairs of microRNAs (Figure 4). For each pair of microRNAs, a threshold was determined on the ratio of the expression levels of the two microRNAs (*Materials and Methods*)—this is equivalent to a straight line that separates two regions in log-space (see Figure 4). In the first step (Figure 4B), if the ratio of relative expression (normalized fluorescence) of hsa-miR-221 to relative expression (normalized fluorescence) of hsa-miR-210 is greater than the threshold value of 9.86, the sample takes the left branch (Figure 4A) and is identified as either oncocytoma or chromophobe. If (hsa-miR-221/hsa-miR-210)<9.86, the samples takes the right branch (gray shaded region in Figure 4B) and is identified as either conventional or papillary. In the second step, the

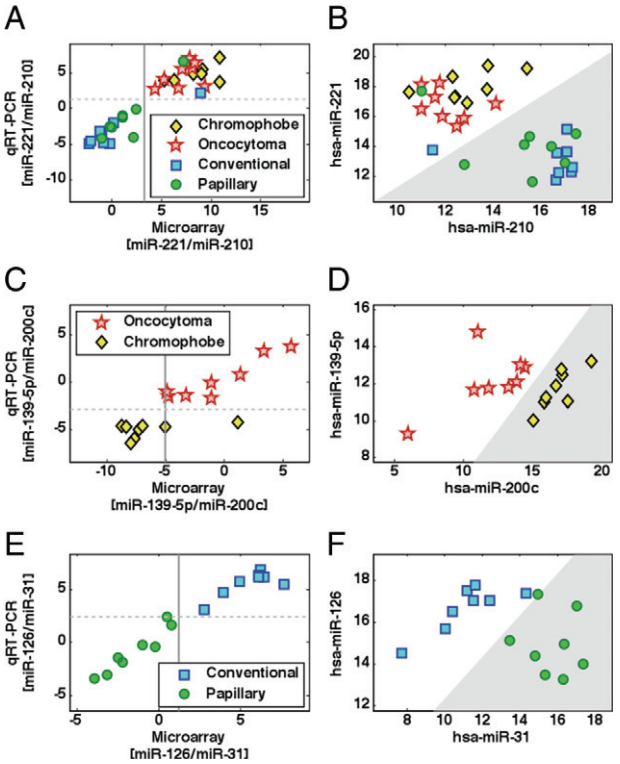

Figure 5. Validation by qRT-PCR. The qRT-PCR validation set included 32 tumor samples: 8 oncocytoma tumors (red stars), 8 chromophobe tumors (yellow diamonds), 8 conventional tumors (blue squares), and 8 papillary tumors (green circles). For each decision point (Figure 4A), the plot on the left side (**A**, **C**, or **E**) shows the log2 expression ratio of the two microRNAs used at this node as measured by microarray (horizontal, calculated as the log2 ratio of the normalized fluorescence signal) and by qRT-PCR (vertical, calculated as the difference in normalized Ct values). In each plot, the vertical line demarcates the classification threshold trained on the microarray data, while the horizontal line indicates the classification threshold that was chosen for the qRT-PCR data, based on the microarray threshold (Methods). The plots on the right side (**B**, **D**, or **F**) show the qRT-PCR data (normalized Cts) of the two microRNAs in the samples of the relevant subtypes at each node. The gray shaded regions indicate the thresholds for classification for each pair of microRNAs, indicating in each case the right branch in the binary classification tree (Figure 4A). **A:** Log2 expression ratio of [hsa-miR-221/hsa-miR-210] in microarray and qRT-PCR. Correlation coefficient was 0.92. **B:** Normalized Cts of hsa-miR-221 and hsa-miR-210 in 32 samples. **C:** Log2 expression ratio of [hsa-miR-139-5p/hsa-miR-200c] in microarray and qRT-PCR. Correlation coefficient was 0.86. **D:** Normalized Cts of hsa-miR-139-5p and hsa-miR-200c in 16 oncocytoma and chromophobe samples. **E:** Log2 expression ratio of [hsa-miR-126/hsa-miR-31] in microarray and qRT-PCR. Correlation coefficient was 0.98. **F:** Normalized Cts of hsa-miR-126 and hsa-miR-31 in 16 conventional and papillary samples.

same process is used—if (hsa-miR-200c/hsa-miR-139-5p)>33.1, the sample is classified as chromophobe (gray region in Figure 4C), otherwise it is classified as oncocytoma. Alternatively, if (hsa-miR-126/hsa-miR-31)<2.32, the sample is classified as papillary (gray region in Figure 4D), otherwise it is classified as conventional. In the training set, this classifier correctly identified 62 of 71 samples, with an overall accuracy of 87% (95% confidence interval: 77–94%, assuming a binomial distribution).

Samples from 54 independent cases were collected as a test set (Figure 4). These samples were processed and their microRNA expression profiles were measured using the same protocols, more than two months after the initial training set samples were profiled. The microRNA expression profiles of these samples were used to predict their histological subtype according to the classification algorithm defined above (Figure 4). Of the 54 test samples, 50 samples were classified correctly and four samples were classified incorrectly (Table 3): two of the 14 chromophobe samples were classified as oncocytoma; one of the 17 oncocytoma samples was classified as chromophobe; one of the 17 conventional samples was classified as oncocytoma; the remaining 50 samples including all six papillary samples were classified correctly. Identification sensitivity was 94% for oncocytoma, 86% for chromophobe, 94% for conventional, and 100% for papillary, with overall accuracy of 93% (95% confidence interval: 82–98%, assuming a binomial distribution).

To validate the classifier using a different platform, 32 samples (eight from each subtype) from both the training set (17 samples) and the test set (15 samples), were randomly chosen and the six classifier microRNAs were measured using qRT-PCR (*Materials and Methods*). qRT-PCR results demonstrated high correlation with microarray results for the expression ratios of hsa-miR-221/hsa-miR-210, hsa-miR-200c/hsa-miR-139-5p, and hsa-miR-126/hsa-miR-31 (Figure 5, A, C, and E) with correlation coefficients of 0.92, 0.86, and 0.98, respectively. Thresholds for the classification using the qRT-PCR data were chosen based on the thresholds trained on the microarray data (*Materials and Methods*). Of these samples, 91% (93% of the test set samples) were classified correctly by the qRT-PCR data (Figure 5, B, D, and F, and Table 3). Thirty of the 32 samples were classified by the qRT-PCR in agreement with the classification using microarray. Two cases showed disagreement between the two platforms: one chromophobe tumor sample that was misclassified as oncocytoma in the microarray was classified correctly as chromophobe in the qRT-PCR (Figure 5C). One papillary tumor sample correctly identified by the microarray classifier was misclassified as conventional type by the qRT-PCR classifier (Figure 5E). The expression ratios for this latter sample were close to the classification threshold in both platforms.

Discussion

Renal cell cancer comprises different subtypes of cancers that differ in genetic background, responses to surgical and medical therapy, and prognoses. The different histological subclasses of RCC are associated with the different disease specific survival that range from 24% to 100% at 5 years from surgery.[8–11] While nonconventional types of RCC have a lower pathological stage and reduced portion of metastatic disease, its response to systemic medical therapy is reduced compared with conventional type RCC.[17] A postoperative prediction nomogram to predict the probability for recurrence following surgical therapy used histology subtyping in addition to the preoperative patient's symptoms, tumor size, and pathological stage.[42] Various markers have been suggested and used for this distinction between histology subtypes, but these show mixed or limited specificities, and a significant fraction of samples may be unclassified or misclassified.[10,43,44] Unclassified RCC comprise up to 6% of all RCC even in series from centers of excellence and have the worst clinical outcome as compared with other subclasses.[8,45,46] We can assume that the

Table 2. Association between Coexpressed MicroRNAs and Their Predicted Coregulating Transcription Factors (TFs)

Transcription factor(s)	MicroRNAs with predicted TF binding sites
MicroRNAs upregulated in oncocytoma	
Ahr,Arnt, GR-alpha, GR-beta	hsa-miR-139-5p, hsa-miR-365
MicroRNAs upregulated in oncocytoma and chromophobe tumors	
AR,Arnt, MEF-2A, NCX	hsa-miR-10a and hsa-miR-221/222
Cdc5, POU3F2 (N-Oct-5a), POU3F2 (N-Oct-5b)	hsa-miR-182, hsa-miR-221/222
c-Myc, Max1, SREBP-1a (b,c)	hsa-miR-10a, hsa-miR-30b
E4BP4, Hlf	hsa-miR-221/222, hsa-miR-30b
GATA-1, MZF-1	hsa-miR-10a, hsa-miR-182
LCR-F1	hsa-miR-182, hsa-miR-221/222, hsa-miR-30b
POU3F2, TBP	hsa-miR-10a, hsa-miR-182, hsa-miR-221/222
MicroRNAs upregulated in papillary tumors	
AREB6	hsa-miR-196b, hsa-miR-200a/b, hsa-miR-31
C/EBPbeta	hsa-miR-196b, hsa-miR-31
HNF-1A	hsa-miR-200a/b, hsa-miR-31
POU2F1, Sp1, SRF, YY1	hsa-miR-196b, hsa-miR-200a/b
MicroRNAs upregulated in conventional and papillary tumors	
AhR, AP-4, Arnt	hsa-miR-192/4, hsa-miR-210, hsa-miR-455-3p
AP-2alphaA, AP-2gamma	hsa-miR-21, hsa-miR-210, hsa-miR-455-3p
AR, AREB6, Nkx2-1	hsa-miR-192/4, hsa-miR-204
ATF6	hsa-miR-192/4, hsa-miR-455-3p
E47	hsa-miR-192/4, hsa-miR-204, hsa-miR-455-3p
Elk-1	hsa-miR-204, hsa-miR-21
AP-2rep, FOXD1, MAZR	hsa-miR-204, hsa-miR-210
GATA-1, NF-kappaB2, Sox9	hsa-miR-146a, hsa-miR-204
GR-alpha	hsa-miR-210, hsa-miR-455-3p
HSF1 (long), Meis-1	hsa-miR-146a, hsa-miR-204, hsa-miR-210
HSF2, OCA-B, Octa-factor, octamer-binding factor, Oct-B1(B2, B3), POU2F2 (2F2B, 2F2C, 3F1, 3F2, 4F1(l), 5F1A, 5F1B, 5F1C)	hsa-miR-146a, hsa-miR-210
ISGF-3, Pax-5, STAT1alpha, STAT1beta, STAT3	hsa-miR-204, hsa-miR-455-3p
MEF-2A	hsa-miR-146a, hsa-miR-21, hsa-miR-455-3p
NF-kappaB, NF-kappaB1	hsa-miR-146a, hsa-miR-192/4, hsa-miR-204, hsa-miR-455-3p
Pax-2	hsa-miR-192/4, hsa-miR-204, hsa-miR-210, hsa-miR-455-3p
POU2F1	hsa-miR-146a, hsa-miR-192/4, hsa-miR-204, hsa-miR-210
PPAR-gamma1, PPAR-gamma2	hsa-miR-192/4, hsa-miR-204, hsa-miR-210
RelA	hsa-miR-146a, hsa-miR-192/4, hsa-miR-455-3p

MicroRNAs were clustered according to a similar expression pattern across the four different renal tumor types as described in Figure 2. TFs were associated with microRNAs following existence of predicted TF binding sites in the microRNA promoter as described.[40] The table lists only TFs which were associated with at least two coexpressed microRNAs. Several TFs in the same row indicate that all TFs are associated with the same microRNAs in that row. MicroRNAs presented as hsa-miR-###/# (eg, hsa-miR-192/4), indicate that the two microRNAs are located in the same genomic cluster and therefore are predicted to be part of a shared pri-microRNA. KIT is not represented in the table as it is associated with hsa-miR-221/222 but not coexpressed microRNA.

proportion of unclassified RCC is higher in centers lacking dedicated pathologists focusing in genitourinary malignancies, therefore emphasizing the need for additional diagnostic tools for RCC subclassification.

Here we investigated the utility of microRNA as potential biomarkers for the identification of these distinct biological entities. We identified a set of microRNAs that are significantly differentially expressed between the four common types of renal malignancies. MicroRNA expression profiles exhibited an underlying similarity between oncocytoma and chromophobe, and between conventional and papillary tumors, reflecting their distinct biological origins.[14] We designed a diagnostic algorithm that takes advantage of this similarity and distinguishes between RCC subtypes based on the expression of six microRNAs. The gold standard used in this study was

Table 3. Classification of Renal Tumors Using Expression Levels of 6 MicroRNAs

	Classification based on microarray data in the test set				
Reference diagnosis	Oncotcytoma	Chromophobe	Conventional	Papillary	Correct classifications
Oncotcytoma	16	1	—	—	16/17 (94%)
Chromophobe	2	12	—	—	12/14 (86%)
Conventional	1	—	16	—	16/17 (94%)
Papillary	—	—	—	6	6/6 (100%)
Classification based on qRT-PCR data					
Oncotcytoma	8 (4)	—	—	—	8/8 (4/4)
Chromophobe	—	8 (4)	—	—	8/8 (4/4)
Conventional	1 (-)	—	7 (4)	—	7/8 (4/4)
Papillary	—	1 (-)	1 (1)	6 (2)	6/8 (2/3)

The upper part of the table shows the classification results for the 54 microarray test set samples (Figure 4). The lower part of the table shows the classification results for 32 samples measured by qRT-PCR. Eight samples chosen randomly from each group were measured by proprietary microRNA qRT-PCR for the six microRNAs used in the classification (Figure 5). The table shows the number of samples from each group that were classified into each predicted class (*Materials and Methods*). Numbers in parentheses (in the qRT-PCR section) indicate the values for the test-set samples.

histolopathologic classification based on pathological review, which can have significant observer variability.[10,47] Furthermore, the classification algorithm developed on microarrays used only microRNA markers and did not use other potential markers. Nevertheless, the microRNA-based classifier we developed reached an accuracy of 93% in histological classification of an independent set of 54 test samples. We validated this classifier on a qRT-PCR platform[30,48] and demonstrated that renal tumor subtypes can be accurately identified using qRT-PCR measurement for the set of six specific microRNA markers. The results obtained using microarray expression profiling compare favorably with classification accuracy of 78–87% obtained using IHC markers[24] and can provide additional information for characterization of nondiagnostic biopsies.[27] Furthermore, classification rules based on quantitative measurement of microRNA expression levels can form a basis for standardized objective assays.[30,48,49] This diagnostic model based on microRNA expression levels can potentially be used to complement existing tools at preoperative and postoperative setting to differentiate the four major RCC subtypes and may be a useful clinical aid for the diagnosis and management of renal tumor cases.

The differentially expressed microRNAs we identified can provide clues to the biological differences between the subtypes, their diverging oncogenetic processes, and possible new targets for type-specific target therapy. We found that hsa-miR-141 and hsa-miR-200c are specifically expressed in the chromophobe tumors—this agrees with a previous study that found these microRNAs down-regulated in conventional tumors.[35] This family of microRNAs is strongly expressed in epithelial tissues[31] and is involved in the regulation of the epithelial-to-mesenchymal transition.[50,51,52] Hsa-miR-221 and hsa-miR-222 are strongly expressed in both chromophobe and oncocytoma types. Overexpression of these microRNAs in chromophobe tumors was also observed by Nakada and colleagues.[35] These microRNAs inhibit erythropoiesis by targeting and down-regulating the KIT receptor.[53] Interestingly, KIT was found to be expressed specifically in oncocytoma and chromophobe subtypes of RCC[54–57]—the interplay between hsa-miR-221/222 and KIT in renal cells and its contribution to renal malignancies remains to be studied. Other microRNAs show strong differences in expression between the subtypes (Table 1), but their involvement in the oncogenic process is not clear. Some clues or links to other known pathways may be found through transcription factors that potentially regulate these microRNAs (Table 2).[40] Further research will be required to elucidate the biological mechanisms these regulate, and how these can be used for future therapeutic approaches.

Acknowledgments

We thank Jung-Hwan Yoon (Seoul National University College of Medicine) and Netta Sion Vardy (Soroka University Medical Center) for their assistance. We thank technicians and researchers at Rosetta Genomics for their assistance and contributions.

References

1. Jemal A, Siegel R, Ward E, Hao Y, Xu J, Murray T, Thun MJ. Cancer statistics, 2008. CA Cancer J Clin 2008, 58:71–96
2. Hollingsworth JM, Miller DC, Daignault S, Hollenbeck BK. Rising incidence of small renal masses: a need to reassess treatment effect. J Natl Cancer Inst 2006, 98:1331–1334
3. Jemal A, Siegel R, Ward E, Murray T, Xu J, Smigal C, Thun MJ. Cancer statistics, 2006. CA Cancer J Clin 2006, 56:106–130
4. Chow WH, Devesa SS, Warren JL, Fraumeni JF Jr. Rising incidence of renal cell cancer in the United States. JAMA 1999, 281:1628–1631
5. Chow WH, Linehan WM, Devesa SS. Re: Rising incidence of small renal masses: a need to reassess treatment effect. J Natl Cancer Inst 99, 569–570; author reply 2007, 570–561
6. Aben KK, Luth TK, Janssen-Heijnen ML, Mulders PF, Kiemeney LA, van Spronsen DJ. No improvement in renal cell carcinoma survival: a population-based study in the Netherlands. Eur J Cancer 2008, 44:1701–1709
7. Russo P, Jang TL, Pettus JA, Huang WC, Eggener SE, O'Brien MF, Karellas ME, Karanikolas NT, Kagiwada MA. Survival rates after resection for localized kidney cancer: 1989 to 2004. Cancer 2008, 113:84–96
8. Amin MB, Tamboli P, Javidan J, Stricker H, de-Peralta Venturina M, Deshpande A, Menon M. Prognostic impact of histologic subtyping of adult renal epithelial neoplasms: an experience of 405 cases. Am J Surg Pathol 2002, 26:281–291
9. Cheville JC, Lohse CM, Zincke H, Weaver AL, Blute ML. Comparisons of outcome and prognostic features among histologic subtypes of renal cell carcinoma. Am J Surg Pathol 2003, 27:612–624
10. Ficarra V, Martignoni G, Galfano A, Novara G, Gobbo S, Brunelli M, Pea M, Zattoni F, Artibani W. Prognostic role of the histologic subtypes of renal cell carcinoma after slide revision. Eur Urol 2006, 50:786–793; discussion 793–784
11. Mancini V, Battaglia M, Ditonno P, Palazzo S, Lastilla G, Montironi R, Bettocchi C, Cavalcanti E, Ranieri E, Selvaggi FP. Current insights in renal cell cancer pathology. Urol Oncol 2008, 26:225–238
12. Eble JN, Sauter G, Epstein JI, Sesterhenn IA. World Health Organization classification of tumours. IARC Press, Lyon, 2004, pp. 9–87
13. Nagashima Y, Inayama Y, Kato Y, Sakai N, Kanno H, Aoki I, Yao M. Pathological and molecular biological aspects of the renal epithelial neoplasms, up-to-date. Pathol Int 2004, 54:377–386
14. Lam JS, Leppert JT, Figlin RA, Belldegrun AS. Role of molecular markers in the diagnosis and therapy of renal cell carcinoma. Urology 2005, 66:1–9
15. Linehan WM, Walther MM, Zbar B. The genetic basis of cancer of the kidney. J Urol 2003, 170:2163–2172
16. Lopez-Beltran A, Kirkali Z, Cheng L, Egevad L, Regueiro JC, Blanca A, Montironi R. Targeted therapies and biological modifiers in urologic tumors: pathobiology and clinical implications. Semin Diagn Pathol 2008, 25:232–244
17. Motzer RJ, Bacik J, Mariani T, Russo P, Mazumdar M, Reuter V. Treatment outcome and survival associated with metastatic renal cell carcinoma of non-clear-cell histology. J Clin Oncol 2002, 20:2376–2381
18. Motzer RJ, Hutson TE, Tomczak P, Michaelson MD, Bukowski RM, Rixe O, Oudard S, Negrier S, Szczylik C, Kim ST, Chen I, Bycott PW, Baum CM, Figlin RA. Sunitinib versus interferon alfa in metastatic renal-cell carcinoma. N Engl J Med 2007, 356:115–124
19. Mostofi, Sesterhenn & Sobin. Histological typing of kidney tumors. Geneva World Health Organization 1981, 25:1–23
20. Kopper L, Timar J. Genomics of renal cell cancer– does it provide breakthrough? Pathol Oncol Res 2006, 12:5–11
21. Delahunt B, Eble JN, McCredie MR, Bethwaite PB, Stewart JH, Bilous AM. Morphologic typing of papillary renal cell carcinoma: comparison of growth kinetics and patient survival in 66 cases. Hum Pathol 2001, 32:590–595
22. Kovacs G, Wilkens L, Papp T, de Riese W. Differentiation between papillary and nonpapillary renal cell carcinomas by DNA analysis. J Natl Cancer Inst 1989, 81:527–530
23. Tickoo SK, Lee MW, Eble JN, Amin M, Christopherson T, Zarbo RJ,

Amin MB. Ultrastructural observations on mitochondria and microvesicles in renal oncocytoma, chromophobe renal cell carcinoma, and eosinophilic variant of conventional (clear cell) renal cell carcinoma. Am J Surg Pathol 2000, 24:1247–1256
24. Allory Y, Bazille C, Vieillefond A, Molinie V, Cochand-Priollet B, Cussenot O, Callard P, Sibony M. Profiling and classification tree applied to renal epithelial tumours. Histopathology 2008, 52:158–166
25. Liu L, Qian J, Singh H, Meiers I, Zhou X, Bostwick DG. Immunohistochemical analysis of chromophobe renal cell carcinoma, renal oncocytoma, and clear cell carcinoma: an optimal and practical panel for differential diagnosis. Arch Pathol Lab Med 2007, 131:1290–1297
26. Young AN, Amin MB, Moreno CS, Lim SD, Cohen C, Petros JA, Marshall FF, Neish AS. Expression profiling of renal epithelial neoplasms: a method for tumor classification and discovery of diagnostic molecular markers. Am J Pathol 2001, 158:1639–1651
27. Shannon BA, Cohen RJ, de Bruto H, Davies RJ. The value of preoperative needle core biopsy for diagnosing benign lesions among small, incidentally detected renal masses. J Urol 2008, 180:1257–1261; discussion 1261
28. Bartel DP. MicroRNAs: genomics, biogenesis, mechanism, and function. Cell 2004, 116:281–297
29. Bishop JA, Benjamin H, Cholakh H, Chajut A, Clark DP, Westra WH. Accurate classification of non-small cell lung carcinoma using a novel microRNA-based approach. Clin Cancer Res 2010, 16:610–619
30. Lebanony D, Benjamin H, Gilad S, Ezagouri M, Dov A, Ashkenazi K, Gefen N, Izraeli S, Rechavi G, Pass H, Nonaka D, Li J, Spector Y, Rosenfeld N, Chajut A, Cohen D, Aharonov R, Mansukhani M. Diagnostic assay based on hsa-miR-205 expression distinguishes squamous from nonsquamous non-small-cell lung carcinoma. J Clin Oncol 2009, 27:2030–2037
31. Rosenfeld N, Aharonov R, Meiri E, Rosenwald S, Spector Y, Zepeniuk M, Benjamin H, Shabes N, Tabak S, Levy A, Lebanony D, Goren Y, Silberschein E, Targan N, Ben-Ari A, Gilad S, Sion-Vardy N, Tobar A, Feinmesser M, Kharenko O, Nativ O, Nass D, Perelman M, Yosepovich A, Shalmon B, Polak-Charcon S, Fridman E, Avniel A, Bentwich I, Bentwich Z, Cohen D, Chajut A, Barshack I. MicroRNAs accurately identify cancer tissue origin. Nature Biotechnol 2008, 26:462–469
32. Calin GA, Croce CM. MicroRNA signatures in human cancers. Nat Rev Cancer 2006, 6:857–866
33. Gilad S, Meiri E, Yogev Y, Benjamin S, Lebanony D, Yerushalmi N, Benjamin H, Kushnir M, Cholakh H, Melamed N, Bentwich Z, Hod M, Goren Y, Chajut A. Serum microRNAs are promising novel biomarkers. PLoS ONE 2008, 3:e3148
34. Gottardo F, Liu CG, Ferracin M, Calin GA, Fassan M, Bassi P, Sevignani C, Byrne D, Negrini M, Pagano F, Gomella LG, Croce CM, Baffa R. Micro-RNA profiling in kidney and bladder cancers. Urol Oncol 2007, 25:387–392
35. Nakada C, Matsuura K, Tsukamoto Y, Tanigawa M, Yoshimoto T, Narimatsu T, Nguyen LT, Hijiya N, Uchida T, Sato F, Mimata H, Seto M, Moriyama M. Genome-wide microRNA expression profiling in renal cell carcinoma: significant down-regulation of miR-141 and miR-200c. J Pathol 2008, 216:418–427
36. Petillo D, Kort EJ, Anema J, Furge KA, Yang XJ, Teh, B. T. MicroRNA profiling of human kidney cancer subtypes. Int J Oncol 2009, 35:109–114
37. Nass D, Rosenwald S, Meiri E, Gilad S, Tabibian-Keissar H, Schlosberg A, Kuker H, Sion-Vardy N, Tobar A, Kharenko O, Sitbon E, Lithwick Yanai G, Elyakim E, Cholakh H, Gibori H, Spector Y, Bentwich Z, Barshack I, Rosenfeld N. MiR-92b and miR-9/9* are specifically expressed in brain primary tumors and can be used to differentiate primary from metastatic brain tumors. Brain Pathol 2009, 19:375–383
38. Benjamini Y, Hochberg, Y. Controlling the false discovery rate: a practical and powerful approach to multiple testing. J Roy Statist Soc Ser B 1995, 57:289–300
39. Griffiths-Jones S, Grocock RJ, van Dongen S, Bateman A, Enright AJ. miRBase: microRNA sequences, targets and gene nomenclature. Nucleic Acids Res 2006, 34:D140–D144
40. Tzur G, Levy A, Meiri E, Barad O, Spector Y, Bentwich Z, Mizrahi L, Katzenellenbogen M, Ben-Shushan E, Reubinoff BE, Galun E. MicroRNA expression patterns and function in endodermal differentiation of human embryonic stem cells. PLoS ONE 2008, 3:e3726
41. Barshack I, Meiri E, Rosenwald S, Lebanony D, Bronfeld M, Aviel-Ronen S, Rosenblatt K, Polak-Charcon S, Leizerman I, Ezagouri M, Zepeniuk M, Shabes N, Cohen L, Tabak S, Cohen D, Bentwich Z, Rosenfeld N. Differential diagnosis of hepatocellular carcinoma from metastatic tumors in the liver using microRNA expression. Int J Biochem Cell Biol 2009, doi: 10.1016/j.biocel.2009.02.021
42. Kattan MW, Reuter V, Motzer RJ, Katz J, Russo P. A postoperative prognostic nomogram for renal cell carcinoma. J Urol 2001, 166:63–67
43. Skolarus TA, Serrano MF, Berger DA, Bullock TL, Yan Y, Humphrey PA, Kibel AS. The distribution of histological subtypes of renal tumors by decade of life using the 2004 WHO classification. J Urol 2008, 179:439–443; discussion 443–434
44. Karakiewicz PI, Hutterer GC, Trinh QD, Pantuck AJ, Klatte T, Lam JS, Guille F, de La Taille A, Novara G, Tostain J, Cindolo L, Ficarra V, Schips L, Zigeuner R, Mulders PF, Chautard D, Lechevallier E, Valeri A, Descotes JL, Lang H, Soulie M, Ferriere JM, Pfister C, Mejean A, Belldegrun AS, Patard JJ. Unclassified renal cell carcinoma: an analysis of 85 cases. BJU Int 2007, 100:802–808
45. Tickoo SK, Gopalan A. Pathologic features of renal cortical tumors. Urol Clin N Am 2008, 35:551–561
46. Zisman A, Chao DH, Pantuck AJ, Kim HJ, Wieder JA, Figlin RA, Said JW, Belldegrun AS. Unclassified renal cell carcinoma: clinical features and prognostic impact of a new histological subtype. J Urol 2002, 168:950–955
47. Feinstein AR, Gelfman NA, Yesner R. Observer variability in the histopathologic diagnosis of lung cancer. Am Rev Respir Dis 1970, 101:671–684
48. Rosenwald S, Gilad S, Benjamin S, Lebanony D, Dromi N, Faerman A, Benjamin H, Tamir R, Ezagouri M, Goren E, Barshack I, Nass D, Tobar A, Feinmesser M, Rosenfeld N, Leizerman I, Ashkenazi K, Spector Y, Chajut A, Aharonov R. Validation of a microRNA-based qRT-PCR test for accurate identification of tumor tissue origin. Mod Pathol 2010, 23:814–823
49. Mansukhani M, Rosenfeld N. Reply to G. Rossi et al. J Clin Oncol 2009, 27:e143–e144
50. Gregory PA, Bert AG, Paterson EL, Barry SC, Tsykin A, Farshid G, Vadas MA, Khew-Goodall Y, Goodall GJ. The miR-200 family and miR-205 regulate epithelial to mesenchymal transition by targeting ZEB1 and SIP1. Nat Cell Biol 2008, 10:593–601
51. Korpal M, Lee ES, Hu G, Kang Y. The miR-200 family inhibits epithelial-mesenchymal transition and cancer cell migration by direct targeting of E-cadherin transcriptional repressors ZEB1 and ZEB2. J Biol Chem 2008, 283:14910–14914
52. Park SM, Gaur AB, Lengyel E, Peter ME. The miR-200 family determines the epithelial phenotype of cancer cells by targeting the E-cadherin repressors ZEB1 and ZEB2. Genes Dev 2008, 22:894–907
53. Felli N, Fontana L, Pelosi E, Botta R, Bonci D, Facchiano F, Liuzzi F, Lulli V, Morsilli O, Santoro S, Valtieri M, Calin GA, Liu CG, Sorrentino A, Croce CM, Peschle C. MicroRNAs 221 and 222 inhibit normal erythropoiesis and erythroleukemic cell growth via kit receptor down-modulation. Proc Natl Acad Sci USA 2005, 102:18081–18086
54. Kruger S, Sotlar K, Kausch I, Horny HP. Expression of KIT (CD117) in renal cell carcinoma and renal oncocytoma. Oncology 2005, 68:269–275
55. Li G, Gentil-Perret A, Lambert C, Genin C, Tostain J. S100A1 and KIT gene expressions in common subtypes of renal tumours. Eur J Surg Oncol 2005, 31:299–303
56. Huo L, Sugimura J, Tretiakova MS, Patton KT, Gupta R, Popov B, Laskin WB, Yeldandi A, Teh BT, Yang XJ. C-kit expression in renal oncocytomas and chromophobe renal cell carcinomas. Hum Pathol 2005, 36:262–268
57. Pan CC, Chen PC, Chiang, H. Overexpression of KIT (CD117) in chromophobe renal cell carcinoma and renal oncocytoma. Am J Clin Pathol 2004, 121:878–883